Development of a Helical Lamb Wave Electromagnetic Acoustic Transducer for Pipe Inspection

Zhe Wang, Shen Wang, Qing Wang, Senior Member, Wei Zhao, and Songling Huang, *Senior Member, IEEE*

***Abstract*—The electromagnetic ultrasonic testing presents great potential in structural health monitoring due to its non-contact advantage. The electromagnetic acoustic transducers generating torsional and longitudinal guided wave have been extensively studied for pipeline structure. However, the transducer for helical wave and corresponding analysis still have not been adequately investigated. This paper proposes the novel transducer to generate helical Lame wave in pipeline. Based on the Lorentz mechanism, the developed transducer contains the fan-shaped magnetic poles and a two-layer coil. The finite element model is built to simulate the wave generation and propagation from the transducer. The displacement distribution verifies the capacity of generating helical wave. The excitation and reception of helical wave are also carried out in the experiment. The actual frequency of the transducer measured from the frequency-sweeping coincides with the designed value. In addition, the defect detection experiment is conducted. The axial and circumferential location can be obtained according to the amplitude and time information. The further comparison and discussion indicate that the prior transducer with meander coil is not appropriate to generate helical wave. The developed transducer can generate wave with diverse incident angle which is superior than the transducer for torsional and longitudinal modes.**

***Index Terms*— Guided wave, Lorentz force, pipeline inspection, structural health, transducer.**

I. Introduction

The structural health monitoring (SHM) is vital for damage prognosis. The techniques of passive and active SHM hav been investigated to monitor the structural integrity[1]. The passive SHM could utilize the acoustic emission from the structure through applying the embedded sensors [2], [3]. The active SHM transmits ultrasonic waves into the structure and records the responses [4], [5]. The guided wave active SHM provides an effective method for the rapid inspection of pipelines 6[] – [9]. Compared with ultrasound bulk wave, guided wave is capable of propagating a longer distance in the inspected objects with little energy loss. The guided wave can be generated by piezoelectric transducer and electromagnetic acoustic transducer (EMAT) [10]. The piezoelectric transducer is required to contact the objects with coupling medium, while EMAT has the advantage of non-contact nature which extends its range of applications [11]. However, the energy conversion efficiency of EMAT is rather low and thus the signal-to-noise ratio need to be improved.

Two mechanisms of Lorentz force and magnetostrictive effect have mainly been utilized in the transduction process of EMAT. For the Lorentz force mechanism, the permanent magnets and coil are usually applied to generate the bias magnetic field and dynamic magnetic field, respectively [12]. For magnetostrictive effect, the deformation in ferromagnetic material will occur when outer magnetic field is imposed [13]. The performances of different EMAT configurations had been assessed and compared using quantitative measurement [14]. The transducer can generate multiple guided wave modes and the Lamb wave has been extensively investigated to analyze its potential in damage detection. The silicon steel laminations had been applied to increase the efficiency of EMAT by enhance the dynamic magnetic field and eddy current in the sample surface [15]. The omni-directional Lamb-wave was generated by axisymmetrically configured magnetostrictive patch transducer [16]. Further, the magnets in the structure were modified to improve the signal [17]. The high-order Lamb wave modes were also generated based on the inclined magnetic field because the higher modes own better detection sensitivity [18]. To understand the Lamb wave signal, the Lamb wave propagation analysis and interaction with damage had been conducted in numerical simulation and experimental validation [19], [20].

The guided wave in pipeline can propagate in the circumferential, axial and helical direction [21]-[24]. Multiple structural designs of transducers for the axial guided wave including torsional mode and longitudinal mode had been reported in the literatures [25], [26]. The magnetostrictive transducer using several pieces of nickel strips was proposed to generate torsional mode for the long-term on-line monitoring of buried pipelines [27]. The smart and harmonized flexible printed coil sensor was designed to generate an even magnetostrictive force and thus enhance the ability to detect defects in pipes [28]. However, the axial guided wave propagates in the single direction, which provides the only incident angle to interact with the defect. The information in the received signal is not abundant to identify the circumferential position of defects. Therefore, the scheme to generate multiple directions and dense acoustic ray is needed to accomplish more accurate pipeline inspection. Meanwhile, the number of transducers is required to be rational.

*Correspondence to: Songling Huang. (Email: huangsling@tsinghua.edu.cn) State Key of Power Systems, Department of Electrical Engineering, Tsinghua University, Beijing, 10084, China
Zhe Wang, Shen Wang, Wei Zhao, and Songling Huang are with the State Key Laboratory of Power System, Department of Electrical Engineering, Tsinghua University, Beijing 100084, China
Q. Wang is with the Department of Engineering, Durham University, Durham DH1 3LE, U.K.

The helical Lamb wave propagates along the spiral line around the pipeline which can pass through the inspected region in extra angles [29]. The contact longitudinal transducers utilizing piezoelectric effect had been applied to generate helical Lamb wave [30], [31]. The macro fibers composite sensors containing the piezoceramic fibers had been attached to the hollow cylinder with an angle to the axis to control the propagation direction of the ultrasonic signal [32]. To the best of our knowledge, the exploration of helical Lamb wave is not sufficient. The efficient transducer needs to be designed and characteristic analysis requires to be implemented.

In this work, the EMAT for helical Lamb wave is proposed and corresponding verification is conducted. The Lorentz force mechanism is utilized and the transducer covers part of the pipeline circumference. The transducer is composed of the two-layer coil and fan-shaped magnetic poles. The generated guided wave distributes in a range of angle to form the helically propagated wave. The excitation and propagation are firstly validated in finite element model. Then the experiment is carried out to generate and receive the helical Lamb wave. In addition, the transducer is applied to accomplish the defect localization. The comparison and discussion are also provided combining the analysis of prior transducers.

II. THE DESIGN OF THE PROPOSED EMAT

A. Configuration and Working Principle

The guided wave transducers based on Lorentz force are commonly composed of coils, permanent magnets, and detected objects. The generation of guided wave involves multiphysics coupling, including electromagnetic field, force field, and acoustic field. The configuration of proposed transducer for helical Lamb wave is shown in Fig. 1. The transducer occupies only a portion of the pipeline circumference. Thus, multiple transducer can be distributed along the circumference to form an array which is capable of imaging the inspected area. Fig. 1(b) provides the detailed structure of the developed transducer. The magnetic poles in the shape of sector are adopted to supply the bias magnetic field. The two-layer coil is placed between the magnets and pipeline. The coil is manufactured using the technique of flexible printed circuit board and the lead wire is placed in the two layers. The interval in the coil is designed deliberately to utilize the wave superposition principle. The coil is connected to the high power pulse source which is used to generate high-frequency pulse. In this work, the windowed sinusoidal signal called tone-burst is adopted as the pulse. The alternating magnetic field generated by the high-frequency pulse and the static bias magnetic field from the permanent magnets are imposed on the pipeline. Based on the Lorentz force, the ultrasonic guided wave can be excitated. It is worth to noting that in the ferromagnetic material, the magnetostrictive effect also plays the role in generating guided wave. While, the Lorentz force mechanism is modeled and analyzed in the following part.

If the diameters of the pipeline is far larger than the wavelength and pipe thickness, the pipe structure can be regarded as the lat plate. Thus the theoretical relation in the Lamb wave can be applied in the helical Lamb wave [33], [34]. The route of the

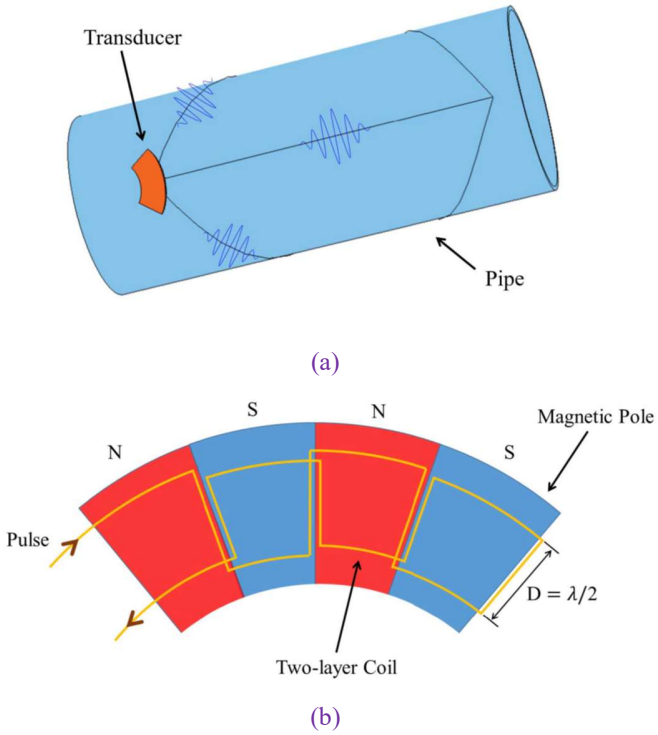

Fig. 1 The designed transducer for helical Lamb wave. (a) The wave propagating in direct and spiral way. (b) The detailed depiction of the transducer structure.

helical Lamb wave propagating spirally around the pipe can be modeled as the direct wave in plate. Lamb wave own two types: symmetric and anti-symmetric modes. They can coexist at any given frequency. The theoretical formula for Lamb wave is known as Rayleigh-Lamb equation. Through solving the equation, the dispersion curve can be obtained. The dispersive characteristic means the velocity of Lamb wave is varied with the changing of excitation frequency and pipe thickness. For the tested steel with material mass density of 7850 k.m^{-3}, Possion's ratio of 0.28 and Yong's modulus of 205GPa, the results of the dispersion curve are presented in Fig. 2. The inclined dashed line in Fig 2(b) indicates the same wavelength since the wavelength is calculated by dividing phase velocity with frequency. It can be used to design the parameters in the transducer.

In the design of the transducer, the interval of the coil denoted as D is the key parameter to decide the wavelength of generated wave. The wave superposition is utilized in the transduction process. Under the magnetic poles, the direction of current in the wire decides the direction of induced eddy current. The magnetic poles bring different direction of magnetic field and thus influence the wave phase. Meanwhile, the spatial positions of wire also lead to the phase difference in generated guided wave. If the distance parameter D in the coil equals to the half of wavelength which is denoted as λ, the wave phase in the inspected region from each magnetic pole will be the integral multiple of 2π and thus the generated wave will be superposed positively. In this way, the wave amplitude would be increased and the signal-to-noise ratio could be improved.

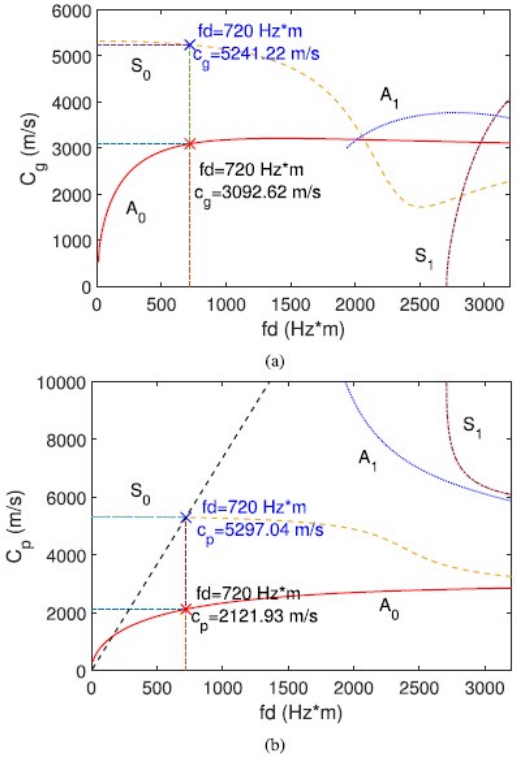

Fig. 2 The dispersion curve from the Rayleigh-Lamb equation. It is the important reference in determining the parameters in transducer. (a) Group velocity. (b) Phase velocity

In this work, the excitation frequency of 120 kHz is chosen and the S0 mode is considered. The thickness and outer diameter of the tested pipeline are 6 and 273 mm, respectively. According the dispersion curve, the phase velocity is 5297.04 m/s and the corresponding wavelength is 44.1 mm. Thus, the spacing in the coil D is 22.05 mm. Since multiple transducers can be placed around the pipeline circumference, eight transducers are considered to form an array. The inner radius and outer radius of each magnetic pole are 30 and 70 mm, respectively. The fan-shaped magnetic pole has the central angle of 20°. Thus, the total central angle of magnets in the transducer is 80°. The larger central angle will generate more diverging wave to propagate in more helical angles.

B. Theoretical Analysis

The excitation of guided wave involves multiple physical field, including the static magnetic field from the magnets, the dynamic magnetic field from pulse current and the force field. According

to Faraday's law of electromagnetic induction, the dynamic magnetic field generated from pulsed current will induce eddy current in the inspected material. The magnetic vector potential induced from the excitation pulse is presented as follows:

$$\frac{1}{\mu}\nabla^2 \boldsymbol{A} - \sigma_e \frac{\partial \boldsymbol{A}}{\partial t} = -\boldsymbol{J}_s \qquad (1)$$

where μ is the magnetic permeability, σ_e is the electrical conductivity, $\boldsymbol{J_s}$ is the source current density and $\boldsymbol{A}$ is the magnetic vector potential. The expression for eddy current density is described as:

$$\boldsymbol{J_e} = -\sigma_e \frac{\partial \boldsymbol{A}}{\partial t}. \qquad (2)$$

The eddy current is distributed in the skin depth of the specimen. Due to the effect of outer magnetic field, the free electron in the eddy current will under the influence of Lorentz force. The expression for Lorentz force is given as follows.

$$\boldsymbol{F_L} = \boldsymbol{J_e} \times \boldsymbol{B} \qquad (3)$$

where $\boldsymbol{F_L}$ is the Lorentz force and $\boldsymbol{B}$ is the outer magnetic field density. The alternating Lorentz force will further lead to the vibration of particles and form the guided wave. The Navier equation describing the elastodynamics mechanism of guided wave is shown as:

$$\nabla \cdot \boldsymbol{\sigma} + \boldsymbol{F_L} = \rho \frac{\partial^2 \boldsymbol{u}}{\partial^2 t^2} \qquad (4)$$

where $\boldsymbol{\sigma}$ is the stress vector, ρ is the material density and $\boldsymbol{u}$ is the displacement vector. The displacements of particles propagate forward with certain energy loss.

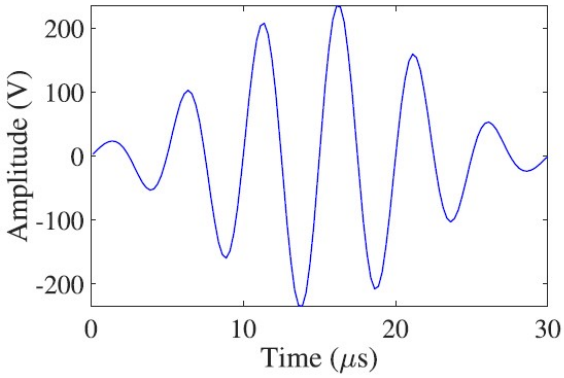

Fig. 3 The illustration of tone-burst. Its frequency and number of cycles is 120 khz and 6, respectively

In the sensor as the wave receiver, the particle vibration under the magnet will generate dynamic current. Moreover, the coil in the sensor will induce electromotive force and the process can be expressed as

$$V = \int_l \boldsymbol{E} \cdot d\boldsymbol{l} \qquad (5)$$

where $\boldsymbol{l}$ is the coil length and $\boldsymbol{E}$ is the electric field generated from the dynamic current. Thus, the ultrasonic signal is converted to electrical signal. The signal is transferred to computer to accomplish further analysis.

III. NUMERICAL SIMULATION

The finite element method is firstly implemented to verify the performance of the designed transducer. The software of COMSOL Multiphysics is adopted because it is suitable to solve the problem with multiple physical fields. The electromagnetic module is applied to simulate the bias and dynamic magnetic

field. The solid structure module is employed to simulate the displacement field due to the Lorentz force. The material and geometrical parameters of the pipeline and the transducer keep the same with those in Section II.

In the simulation, the magnets own the remanent flux density of 0.3 T to provide the bias magnetic field. The tone-burst flowing into the wire can be expressed as:

$$P = A \cdot (0.54 - 0.46\cos(2\pi t/T)) \cdot \sin(2\pi f_c t) \qquad (6)$$

where x, y and z in the subscript indicate the three directions. The mesh size in the model is set far less than the wavelength and in this work the wavelength is 15 times of the mesh size. The time step set in the model is 0.2 μs. The results of the displacement fields from the alternating Lorentz force at different moments are presented in Fig. 4

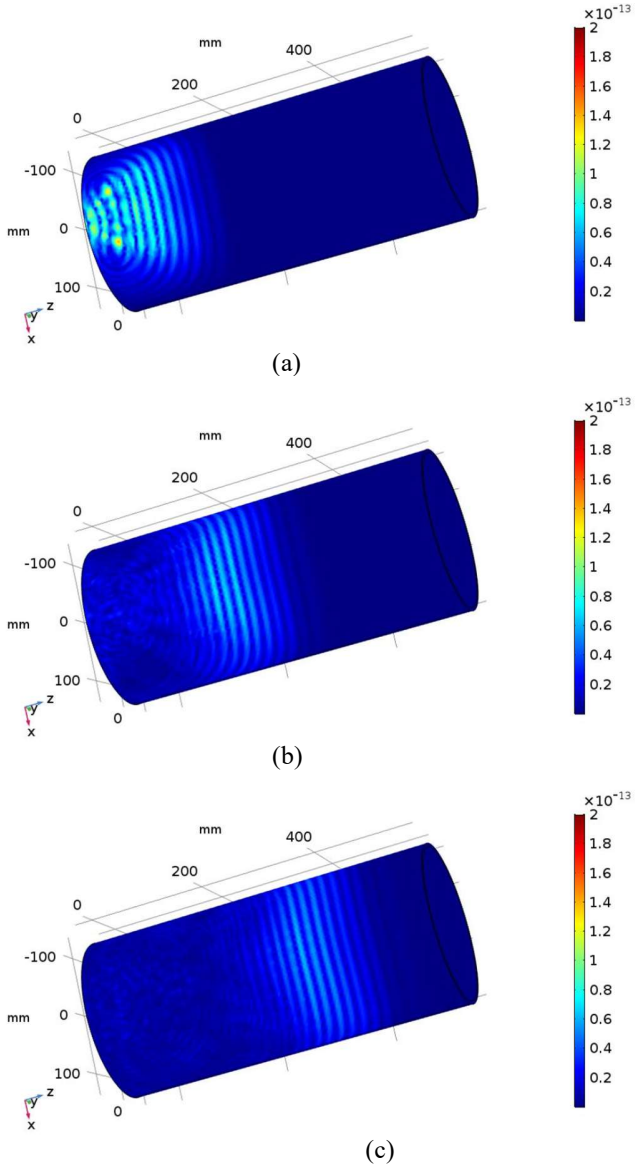

Fig. 4 The helical Lamb wave propagating along the pipeline in the simulation. The displacement fields at (a) 40 μs (b) 70 μs and (c) 100 μs

It can be seen that with the time increases, the helical Lamb wave propagates forward along the pipeline and the acoustic beam also becomes larger. The energy is concentrated at the beginning. With the wave propagation, the energy becomes disperse and the amplitude becomes low. The wave spreads in the circumferential direction of pipeline and thus the wave can propagate spirally with an angle between the route and the pipe axis.

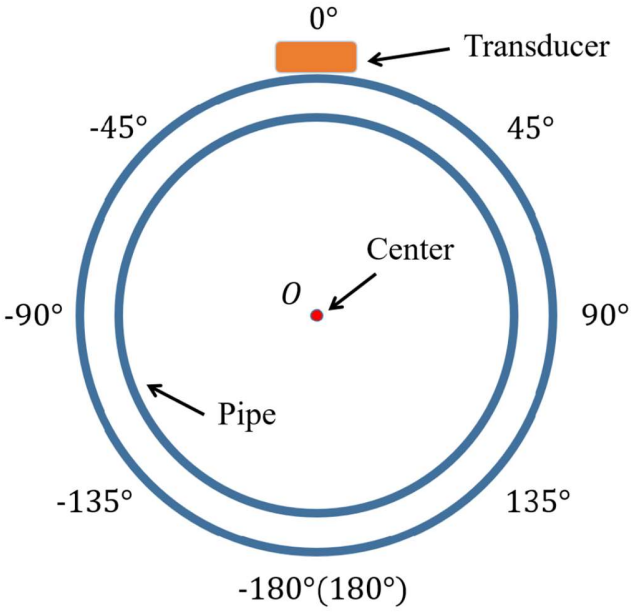

Fig. 5 The illustration of the angular distribution in the pipeline circumference. The position of transducer is defined as 0º.

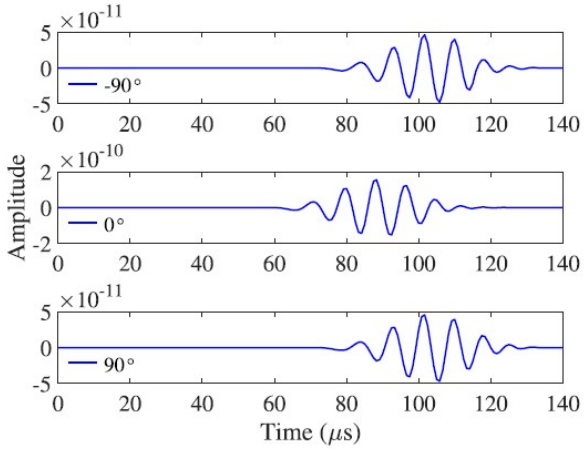

Fig. 6 The obtained displacement waveform from three chosen points in the axial distance of 300mm.

To better understand the propagation characteristic and analyze the defect location, the angular distribution is defined and illustrated in Fig. 5. The circumferential direction of pipeline can be described by the angle. The circumferential position of the transducer is defined as the 0◦. The waveform of three chosen points in the axial distance of 300 mm are shown in Fig. 6. The angles of the three points are −90◦, 0◦ and 90◦. It can be seen that

the arrival time for point of 0° is the earliest because the wave can propagate in a direct line from the excitation point to the receiver point. For points of −90° and 90°, the wave propagate in a helical way and the distance is longer than the direct way. Meanwhile, it can be observed that the wave amplitude of point at −90° is close to that of point at 90°. However, they both are lower than that of point at 0°. Further, the circumferential distribution of peak value from displacement waveform called angular profile is presented in Fig. 7. In each angle, the peak amplitude of displacement is extracted and depicted in the angular profile. The angular profile indicates that the wave energy is concentrated in a certain angle centered on the 0°. The large divergence angle demonstrates that the generated wave will diffuse and propagate in a helical way. Meanwhile, the largest amplitude appears at 0° which is in the direction ahead of the transducer.

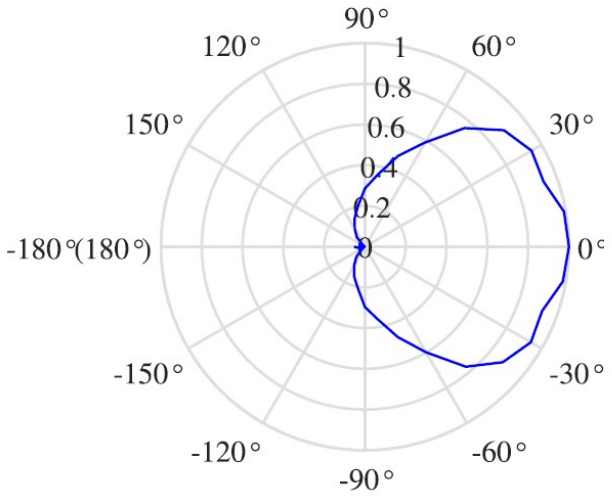

Fig. 7 The angular profile of developed transducer in the axial distance of 300mm.

IV. EXPERIMENTAL INVESTIGATION AND FURTHER DISCUSSION

A. Excitation and Reception of Helical Lamb Wave

The experimental platform is established on the pipeline to validate the developed transducer. The illustration of the experimental system is presented in Fig. 8. The pitch-catch approach is applied and a pair of the transducer is used as the transmitter and receiver. The transmitter was 300 mm away from the receiver in this case. The RITEC RPR-4000 amplifies the signal from the waveform generator to produce the excitation pulse and also receives signals from the receiver. The excitation pulse is a 6-cycle sinusoidal signal windowed by a Hamming function with the center frequency of 120 kHz, which is the same as that in the numerical simulation. The impedance matching is adopted to improve the efficiencies of the transducers. The digital oscilloscope is used to display the waveform and store the data for further analysis.

The average from multiple repeated transmission and reception of helical Lamb wave is conducted to reduce the noise. The received waveforms from three angular positions are shown in Fig. 11. It can be observed that two apparent wavepackets appear in each waveform. The first wavepacket is the main bang which is induced by the receiver coil from the excitation pulse and it is in a synchronized time with the pulse. The second wavepacket is the received wave propagated from the transmitter to the receiver.

To verify the mode of generated wave, the quantitative analysis is employed. For the position at 0°, the propagation distance is the length of the direct line which is 300 mm. For the positions at 90° and −90°, the propagation distance is the length of helical route which can be calculated by expanding the pipe to the flat plate structure and it is 368.7 mm. The timeof- flight of the wavepacket is extracted by using the Hilbert envelope. Then the group velocity can be obtained by the distance divided by the corresponding time-of-flight. Through comparing the calculated group velocity and the theoretical one, the wave mode can be determined. The results are shown in Table I. The last row is the relative error between the
calculated group velocity and that of S_0 mode. The velocities of received wavepackets are consistent with the theoretical values. Therefore, the desired helical S_0 wave is generated.

B. Frequency Response Characteristics

In the designed transducer, the theoretical center frequency of generated wave is correlated with the geometric parameters. As mentioned in Section II-A, the interval in the wire *D* is equal to half wavelength of the desired helical Lamb wave. To test the actual center frequency of the developed transducer, the frequency-sweep experiments are carried out to obtain the frequency response characteristics. The frequency of excitation pulse is increased from 60 kHz to 180 kHz with the increment of 10 kHz. In the experiments, the receiver is set in the front of the transmitter with the axial distance of 300 mm and other factors are kept as the same.

The results are shown in Fig. 10. The polynomial fitting is adopted to analyze the discrete data points. The maximum amplitude is achieved when the frequency equals to 122.1 kHz. Therefore, the measured frequency of the transducer is 122.1 kHz. Combined with the designed frequency of 120 kHz, the relative error can be calculated and it is 1. 75%. The actual frequency is in accordance with the designed value.

C. Defect Inspection Experiment

The main focus of the experiments is to verify the defect detectability of this transducer. One hemispherical defect with radius of 4 mm is machined on the pipeline to simulate the metal loss caused by corrosion. The material and geometrical parameters for the pipeline are the same as the simulation.

The defect scattering is studied in this case. The transmitter and receiver are set in the same side of the defect. The axial distance between the transmitter and the defect is 700 mm. The left and right boundaries are 1000 and 1500 mm away from the transmitter, respectively. The definition of circumferential angle in Fig. 5 is adopted and the defect is located in the angle of 60°. The receiver is 300 mm away from the transmitter along the axial direction. The receiver can be moved around the pipeline circumference and the step size of 45° is applied.

The received waveforms at 0°, 45° and 90° are shown in Fig. 12. Three evident wavepackets can be found in each waveform. Besides the first wavepacket of main bang and the second wavepacket of direct wave, the third one is the reflected wave

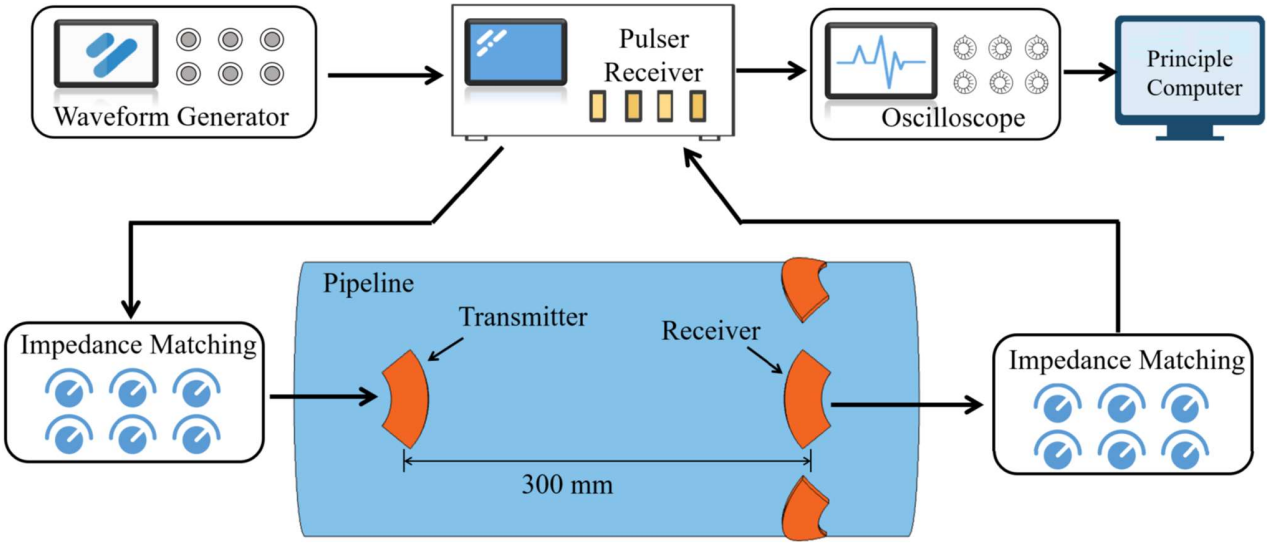

Fig. 8 The schematic diagram of the experimental system for the helical Lamb wave transducer. The pitch-catch approach is applied to inspect the pipeline.

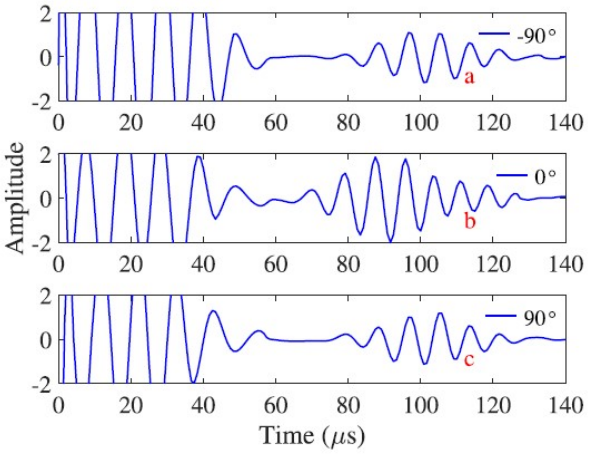

Fig. 9 The received waveform three angular positions in the experiments.

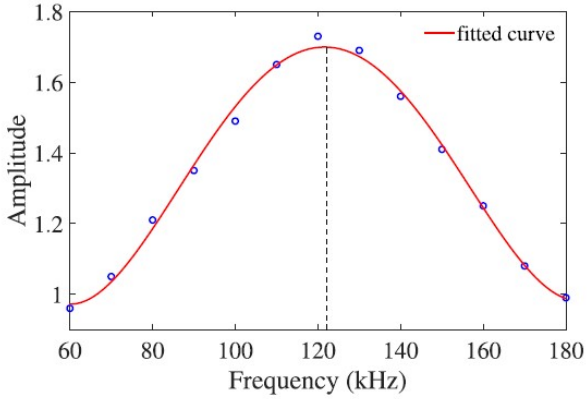

Fig. 10 The result of the frequency sweeping to obtain the frequency response characteristics.

TABLE I
THE RESULTS OF THE QUANTITATIVE ANALYSIS FOR THE WAVEPACKETS OBTAINED IN THE THREE ANGULA POSITIONS

Wavepacket	a	b	c
Time-of-flight (μs)	*69.8*	57.6	69.7
Distance (mm)	*368.7*	300	368.7
Velocity (m/s)	*5282.9*	5208.3	5290.5
Relative error (%)	*0.79*	0.94	0.63

From the defect. Because of the various propagation distances, the arrival times of the wavepackets are different and also the amplitudes.

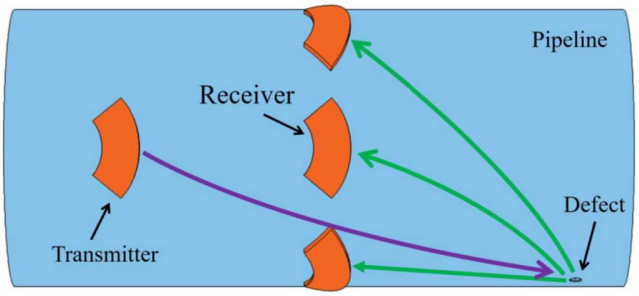

Fig. 11 The illustration of the defect inspection experiment. The transmitter and receiver are set in the same side of defect.

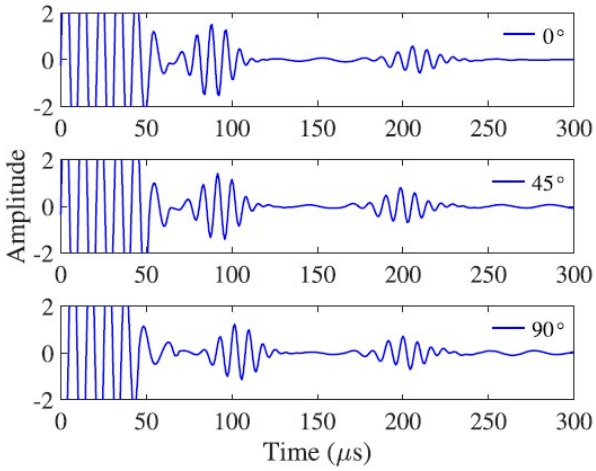

Fig. 12 The received waveforms at 0º, 45º and 90º for the defect detection.

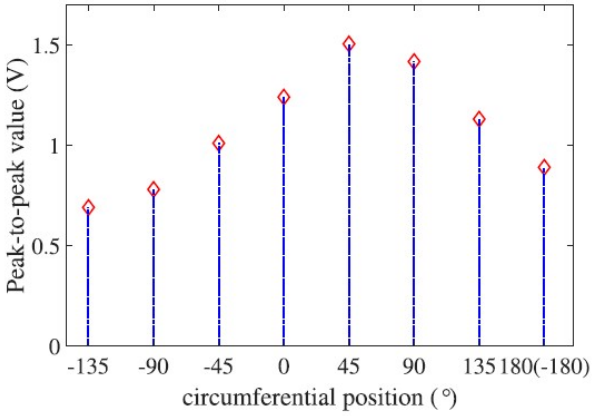

Fig. 13 The peak-to-peak values of defect reflection wavepackets from receiver at the eight circumferential positions.

The waveforms at the eight circumferential positions are obtained and then the peak-to-peak values of wavepackets corresponding to the defect reflection are extracted. The results are presented in Fig. 13. The peak-to-peak values reveal the information of propagation distance which can be used to estimate the circumferential position of defect. The peak-topeak values from receiver in 45◦ and 90◦ show the larger amplitudes than the others. It indicates that the defect is in the circumferential locations between these two angles. Further, the time-of-flight of each wavepacket can be obtained through the hilbert envelope. Combining the geometrical relation, the equations for the axial and circumferential locations can be listed. The accurate locations can be calculated by solving the equations. After the calculation, the axial location of the defect is 713 mm away from the transmitter and the relative error is 1.9 %. It can be inferred that the more accurate time-of-flight extraction method is needed to be developed to improve the localization. The circumferential location of the defect is 54◦. It can be seen that there is a gap between the obtained circumferential location with the actual one. One reason is the transducer owns a certain volume and the received signal is from the entire area under the receiver which brings error in the geometrical relation. The possible alternative scheme is to miniaturize and optimize the transducer.

D. Comparison and Discussion

In this part, the comparisons with prior transducers are conducted. The EAMT composed of magnet and meander coil are commonly used. The corresponding simulations are carried out to obtain the angular profile. The depiction is shown in Fig. 14. The structure of meander coil is also resented. It can be observed that the acoustic field is mainly concentrated on a narrow angle. Therefore, the generated wave will propagate along the straight line ahead of the transmitter and less energy is distributed in the helical direction. The advantage of meander coil is to control the wave mode. However, this transducer is not appropriate to generate helical Lamb wave. The defect in other circumferential angles will be difficult to detect.

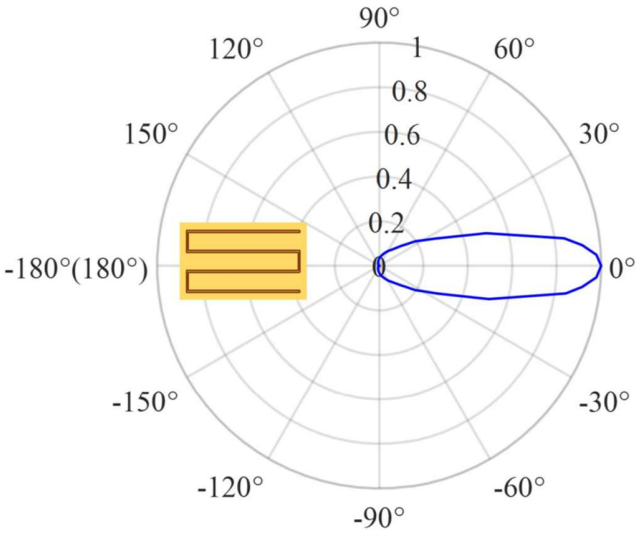

Fig. 14 The angular profile of common used transducer with meander coil.

The transducer covering the whole circumference of pipeline is capable of generating torsional and longitudinal guided wave. Since the excitation is loaded in the range of 360◦ of pipeline, the signal strength can be increased compared with the partial load of the developed transducer. Further, the signal-to-noise ratio can be improved to some extent. The reflection wave can be more easily identified from the noise due to the larger signal amplitude. However, the only axial distance can be deduced from the time information of reflection wave. Besides, the incoming wave owns single incident angle along the axial direction. The developed transducer can generate wave with extra angles to interact with the defect. Although this transducer presents better performance than the prior transducers, the challenge still lies in the practicability when facing actual pipeline. The structure of the designed transducer needs to be adjusted to adapt to pipelines with different diameters. The complexity in the manufacture of the transducer is another nonnegligible factor. Since Lamb wave is considered and generated in this work, the out-of-plane displacement of Lamb wave will lead to the energy leakage into fluid in the pipeline. The leakage will cause shorter propagation distance of guided

wave which is not advantageous for transportation pipeline inspection.

To better exploit the superiority of the designed transducer, the array structure for the transmitter and receiver need to be adopted. Thus, multiple transmissions of helical Lamb wave can be utilized to obtained detailed description of the inspected area. The wave with helical angles can be analysed to extract diverse information. Combining with iterative algorithm, the tomography imaging can be conducted to acquire the outline and depth of the defect. This will be advantageous especially for the pipeline with larger diameter.

V. Conclusions

In this study, a novel transducer for helical wave in pipeline is developed. This transducer includes a two-layer coil and fan-shape magnetic poles. The interval in the coil is utilized to control the wavelength of generated wave. The Lorentz mechanism is modeled to conduct the verification in simulation.

The displacements in three points at -90°, 0° and 90° indicate that the generated wave can propagate in helical way. The angular profile shows that the wave is distributed in a large divergence angle. The corresponding experiments are carried out to validate the excitation and reception of helical Lamb wave. The frequency-sweep shows the actual center frequency agrees with the designed value. The receiver in different circumferential locations perceive the reflection wave from the defect. The peak-to-peak value of wavepacket can be utilized to estimate the circumferential angle of the defect. The accurate axial and circumferential locations can be obtained through building the geometrical equations. The prior transducer with meander coil is capable of generating wave with narrow angle which is not suitable for helical wave. The transducer covering the whole circumference owns better signal strength but it only provides single incident angle. The future work will lie in the further exploitation of this transducer.

References

[1] V. Giurgiutiu, C. Roman, B. Lin, and E. Frankforter, "Omnidirectional piezo-optical ring sensor for enhanced guided wave structural health monitoring," *Smart Mater. Struct.*, vol. 24, no. 1, Jan. 2015, Art. no. 015008.

[2] O. M. Bouzid, G. Y. Tian, K. Cumanan, and D. Moore, "Structural health monitoring of wind turbine blades: Acoustic source localization using wireless sensor networks," *J. Sensors*, vol. 2015, pp. 1–11, Dec. 2015.

[3] S. Masmoudi, A. El Mahi, and S. Turki, "Fatigue behaviour and structural health monitoring by acoustic emission of E-glass/epoxy laminates with piezoelectric implant," *Appl. Acoust.*, vol. 108, pp. 50–58, Jul. 2016.

[4] X. P. Qing *et al.*, "Development of a real-time active pipeline integrity detection system," *Smart Mater. Struct.*, vol. 18, no. 11, Nov. 2009, Art. no. 115010.

[5] Z. Wang, S. Huang, S. Wang, Q. Wang, and W. Zhao, "Multifrequency identification and exploitation in Lamb wave inspection," *IEEE Access*, vol. 7, pp. 150435–150443, 2019.

[6] D. Sen, A. Aghazadeh, A. Mousavi, S. Nagarajaiah, R. Baraniuk, and A. Dabak, "Data-driven semi-supervised and supervised learning algorithms for health monitoring of pipes," *Mech. Syst. Signal Process.*, vol. 131, pp. 524–537, Sep. 2019.

[7] P. Khalili and P. Cawley, "The choice of ultrasonic inspection method for the detection of corrosion at inaccessible locations," *NDT & E Int.*, vol. 99, pp. 80–92, Oct. 2018.

[8] M. Mitra and S. Gopalakrishnan, "Guided wave based structural health monitoring: A review," *Smart Mater. Struct.*, vol. 25, no. 5, May 2016, Art. no. 053001.

[9] Z. Liu and Y. Kleiner, "State-of-the-art review of technologies for pipe structural health monitoring," *IEEE Sensors J.*, vol. 12, no. 6, pp. 1987–1992, Jun. 2012.

[10] R. Guan, Y. Lu, W. Duan, and X. Wang, "Guided waves for damage identification in pipeline structures: A review," *Struct. Control Health Monit.*, vol. 24, no. 11, p. e2007, Nov. 2017.

[11] J. Tkocz, D. Greenshields, and S. Dixon, "High power phased EMAT arrays for nondestructive testing of as-cast steel," *NDT & E Int.*, vol. 102, pp. 47–55, Mar. 2019.

[12] S. Wang, S. Huang, Y. Zhang, and W. Zhao, "Modeling of an omnidirectional electromagnetic acoustic transducer driven by the lorentz force mechanism," *Smart Mater. Struct.*, vol. 25, no. 12, Dec. 2016, Art. no. 125029.

[13] Z. Wei, S. Huang, S. Wang, and W. Zhao, "Magnetostriction-based omni-directional guided wave transducer for high-accuracy tomography of steel plate defects," *IEEE Sensors J.*, vol. 15, no. 11, pp. 6549–6558, Nov. 2015.

[14] R. Ribichini, F. Cegla, P. Nagy, and P. Cawley, "Study and comparison of different EMAT configurations for SH wave inspection," *IEEE Trans. Ultrason., Ferroelectr., Freq. Control*, vol. 58, no. 12, pp. 2571–2581, Dec. 2011.

[15] W. Ren, J. He, S. Dixon, and K. Xu, "Enhancement of EMAT's efficiency by using silicon steel laminations back-plate," *Sens. Actuators A, Phys.*, vol. 274, pp. 189–198, May 2018.

[16] J. K. Lee, H. W. Kim, and Y. Y. Kim, "Omnidirectional Lamb waves by axisymmetrically-configured magnetostrictive patch transducer," *IEEE Trans. Ultrason., Ferroelectr., Freq. Control*, vol. 60, no. 9, pp. 1928–1934, Sep. 2013.

[17] W. Sun, G. Liu, H. Xia, and Z. Xia, "A modified design of the omnidirectional EMAT for antisymmetric Lamb wave generation," *Sens. Actuators A, Phys.*, vol. 282, pp. 251–258, Oct. 2018.

[18] Z. Liu, X. Zhao, J. Li, C. He, and B. Wu, "Obliquely incident EMAT for high-order Lamb wave mode generation based on inclined static magnetic field," *NDT & E Int.*, vol. 104, pp. 124–134, Jun. 2019.

[19] B. C. Lee and W. J. Staszewski, "Modelling of Lamb waves for damage detection in metallic structures: Part I. Wave propagation," *Smart Mater. Struct.*, vol. 12, no. 5, pp. 804–814, Oct. 2003.

[20] B. C. Lee and W. J. Staszewski, "Modelling of Lamb waves for damage detection in metallic structures: Part II. Wave interactions with damage," *Smart Mater. Struct.*, vol. 12, no. 5, pp. 815–824, Oct. 2003.

[21] M. Clough, M. Fleming, and S. Dixon, "Circumferential guided wave EMAT system for pipeline screening using shear horizontal ultrasound," *NDT & E Int.*, vol. 86, pp. 20–27, Mar. 2017.

[22] P. S. Lowe, R. M. Sanderson, N. V. Boulgouris, A. G. Haig, and W. Balachandran, "Inspection of cylindrical structures using the first longitudinal guided wave mode in isolation for higher flaw sensitivity," *IEEE Sensors J.*, vol. 16, no. 3, pp. 706–714, Feb. 2016.

[23] E. Dehghan-Niri and S. Salamone, "A multi-helical ultrasonic imaging approach for the structural health monitoring of cylindrical structures," *Struct. Health Monit.*, vol. 14, no. 1, pp. 73–85, Jan. 2015.

[24] C. L. Willey, F. Simonetti, P. B. Nagy, and G. Instanes, "Guided wave tomography of pipes with high-order helical modes," *NDT & E Int.*, vol. 65, pp. 8–21, Jul. 2014.

[25] Y. Y. Kim and Y. E. Kwon, "Review of magnetostrictive patch transducers and applications in ultrasonic nondestructive testing of waveguides," *Ultrasonics*, vol. 62, pp. 3–19, Sep. 2015.

[26] S. Hill, S. Dixon, S. K. H. Reddy, P. Raiagopal and K. Balasubramaniam, "A new electromagnetic acoustic transducer design for generating torsional guided wave modes for pipe inspections," *AIP Conf.*, vol. 1806, no. 1, 2017, Art. no. 050003.

[27] Y. Y. Kim, C. I. Park, S. H. Cho, and S. W. Han, "Torsional wave experiments with a new magnetostrictive transducer configuration," *J. Acoust. Soc. Amer.*, vol. 117, no. 6, pp. 3459–3468, Jun. 2005.

[28] P. Tse, Z. Fang, and K. Ng, "Novel design of a smart and harmonized flexible printed coil sensor to enhance the ability to detect defects in pipes," *NDT & E Int.*, vol. 103, pp. 48–61, Apr. 2019.

[29] K. R. Leonard and M. K. Hinders, "Guided wave helical ultrasonic tomography of pipes," *J. Acoust. Soc. Amer.*, vol. 114, no. 2, pp. 767–774, Aug. 2003.

[30] K. R. Leonard and M. K. Hinders, "Lamb wave tomography of pipe-like structures," *Ultrasonics*, vol. 43, no. 7, pp. 574–583, Jun. 2005.

[31] A. Balvantin, A. Baltazar, and J.-Y. Kim, "A study of helical Lamb wave propagation on two hollow cylinders with imperfect contact conditions," *AIP Conf.*, vol. 1511, no. 1, pp. 67–74, 2013.

[32] A. Baltazar, E. Rojas, and R. Mijarez, “Structural health monitoring in cylindrical structures using helical guided wave propagation,” *Phys. Procedia*, vol. 70, pp. 686–689, Jan. 2015.

[33] J. Li and J. L. Rose, “Natural beam focusing of non-axisymmetric guided waves in large-diameter pipes,” *Ultrasonics*, vol. 44, no. 1, pp. 35–45, Jan. 2006.

[34] A. Velichko and P.D. Wilcox, “Excitation and scattering of guided waves: Relationships between solutions for plates and pipes,” J. Acoust. Soc. Amer., vol. 125, no. 6, pp.3623-3631, Jun 2009.